J. Fluid Mech. (1974), *vol.* 66, *part* 2, *pp.* 391–415
Printed in Great Britain

Optimal swimming of flagellated micro-organisms

By O. PIRONNEAU† AND D. F. KATZ‡

Department of Applied Mathematics and Theoretical Physics,
University of Cambridge

(Received 13 March 1974)

This paper studies flagellar undulations that propel a micro-organism at a given speed while minimizing its expenditure of hydrodynamical energy. The study is in two basic parts. The first part is a qualitative inquiry into the general nature of undulations that are hydrodynamically optimal in the instantaneous sense. The results indicate that an apparent sliding of the entire flagellum along its instantaneous axis is fundamental to such motions, although an additional deformation is necessary to compensate for the presence of the organism's head. Periodic or semi-periodic undulations are clearly suggested, and must consist of travelling waves propagated in the direction opposite to propulsion.

The second part of the paper is a quantitative inquiry as to the values of parameters that optimize given periodic wave shapes in the time-average sense. The trade-off between wave amplitude and the number of wavelengths is of particular interest. Results are obtained for small amplitude sinusoidal waves and finite amplitude sawtooth waves. For the latter, a single wavelength with amplitude roughly one-sixth of the wavelength is optimal. The significance of the twitching movements of the head is investigated. The results are consistent with the qualitative study and emphasize the need to inhibit such motions. The implications of the dependence of resistive-force coefficients upon wave shape are considered, and the physical significance of rotational pitching motions is assessed.

1. Introduction

The study of the motions of uniflagellated micro-organisms, such as spermatozoa, is an important mechano-chemical problem. Hydrodynamical studies were initiated by Taylor (1951, 1952) and Hancock (1953), and have continued to date. In such studies, a particular active undulation or beat is assigned to the flagellum; the propulsive velocity, rate of working against the surrounding fluid, and distribution of applied viscous bending moments along the flagellum can then be calculated. A knowledge of these bending moments is important when studying the mechanism responsible for the flagellar contraction. Mathematical studies of this nature were initiated by Machin (1958, 1963) and have also progressed to date. In such studies, the internal dynamics of the flagellum are

† Present address: Laboria IRIA, Rocquencourt, 78150 Le Chesnay, France.
‡ Present address: Department of Mechanical Engineering, University of California, Berkeley, U.S.A.

modelled via consideration of the equilibrium between the applied viscous bending moment and an internally induced bending moment. This internal moment, which is decomposed into passive and active effects, physically characterizes the contraction mechanism. The result of such a study is the determination of the flagellar undulations. Thus, studies of the contraction mechanism can be coupled with hydrodynamic determinations of swimming trajectories, e.g. Brokaw (1972).

In this paper, we present a third approach. We start with the fact that an organism is swimming forward at a certain rate, and we inquire as to the most economical way of doing so. The object of this approach is to determine the flagellar undulations responsible for the 'optimal' propulsion. Thus our study is intimately connected with the two previous types of investigations. It would seem reasonable to stipulate that an economical way of swimming is one in which the hydrodynamical energy expenditure by the organism is kept to a minimum. Indeed, this is a problem with which nature was originally faced when designing flagella. Thus our results reflect upon the facility of the evolutionary process, as well as presenting criteria upon which to evaluate the hydrodynamic efficiency of swimming organisms. Of course, when more is understood about the internal mechanics and dynamics of flagella, it may be possible to include specific internal considerations as well. Ideally we might ask, "Given that an organism swims from A to B in a given time, how can the total energy expenditure during this interval be minimized?" This is an optimal control problem of non-standard type,† for which no general theory has been developed. We shall therefore solve an alternative, though closely related problem in which the instantaneous rate of working is minimized at each time.

Throughout the analytical development of the problem we shall use resistive-force theory to describe the propulsive hydrodynamics. That is, we regard the local tangential and normal forces per unit length acting on the flagellum as proportional to the local tangential and normal velocities of the axis of the flagellum, the coefficients of proportionality being the resistance coefficients C_L and C_N, respectively. In the qualitative studies of this paper in §§ 3 and 4, we assume that C_N and C_L are constant. Later, in the quantitative studies of §§ 5, 6 and 7, we consider the dependence of C_N and C_L upon the flagellar wave shape. We shall make use of a complementary resistive-force approximation when considering the influence of the head of an organism. The head contributes a drag force $\mathbf{D}_H$ and moment $\mathbf{M}_H$ to the net viscous reactions acting upon the organism. We assume that $\mathbf{D}_H$ and $\mathbf{M}_H$ depend only upon the movements of the head itself, and that the head is sufficiently symmetrical that its translational and rotational motions are not coupled.‡ Thence we can introduce resistive-force and moment coefficients for the head; throughout this paper we consider an effectively spherical head of radius a. Thus

$$\mathbf{D}_H = C_H \mathbf{v}_H, \quad \mathbf{M}_H = T_H \boldsymbol{\omega}_H, \tag{1.1), (1.2}$$

† The problem is non-standard in the sense of optimal control theory in that the boundaries are not stationary.

‡ This assumption is implicit in the resistive-force treatment of the flagellum.

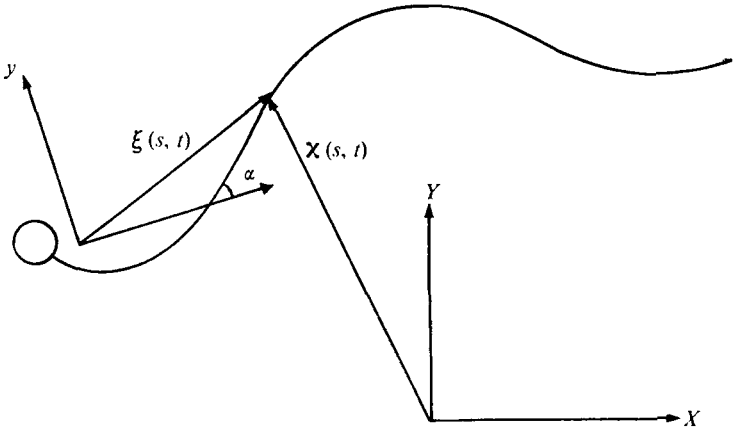

FIGURE 1. $\boldsymbol{\chi}(s, t)$ is the position vector as measured in the fixed X, Y frame of reference. $\boldsymbol{\xi}(s, t)$ is the position vector as measured in the x, y frame moving with the organism.

where $\mathbf{v}_H$ and $\boldsymbol{\omega}_H$ are respectively the absolute linear and angular velocities of the head, and $C_H = 6\pi\mu a$ and $T_H = 8\pi\mu a^3$, the values for an isolated sphere, μ being the viscosity. Despite our analytical use of resistive-force theory, we shall, however, pose the general hydrodynamical problem first, since the applicability of the methods of optimal control theory does not require use of this approximation.

2. Statement of the problem

Our micro-organism is comprised of a deformable flagellum attached to a rigid head. We consider a slender cylindrical flagellum of radius r_0 and length L such that $r_0 \ll L$, and assume that it does not stretch or twist about its local axis. Since all points on a particular cross-section then move with approximately the same velocity,we can describe the motion of the flagellum by the position vector $\boldsymbol{\chi}(s, t)$, with $s \in [0, L]$ and $t \in [0, T]$, to a point M on the axis, where $\boldsymbol{\chi}$ is measured in a co-ordinate system fixed in space (see figure 1). The absolute velocity $\mathbf{v}(s, t)$ of M is given by

$$\mathbf{v}(s, t) = \partial\boldsymbol{\chi}/\partial t = v_l \mathbf{l} + \mathbf{v}_n \mathbf{n}, \tag{2.1}$$

where $\mathbf{l}(s, t)$ and $\mathbf{n}(s, t)$ are respectively the unit forward tangent and normal to the flagellum and, for algebraic clarity, we have considered only two-dimensional flagellar undulations. Thus,

$$\mathbf{l} = \frac{\partial\boldsymbol{\chi}/\partial s}{\|\partial\boldsymbol{\chi}/\partial s\|}, \quad \mathbf{n} = R\,\partial\mathbf{l}/\partial s, \tag{2.2), (2.3}$$

where $R(s, t)$ is the local radius of curvature. The inextensibility condition for the flagellum implies that

$$\partial\|\boldsymbol{\chi}(s+\delta s, t) - \boldsymbol{\chi}(s, t)\|^2/\partial t = 0 \quad \text{for all} \quad s \in [0, L], \quad t \in [0, T]. \tag{2.4}$$

Equation (2.4) yields the relation

$$\partial v_l/\partial s = v_n/R. \tag{2.5}$$

Since the Reynolds number for our swimming micro-organism is extremely small, we can employ the Stokes equations to describe the fluid motions:

$$\mu\nabla^2\mathbf{u} = \nabla p, \quad \nabla.\mathbf{u} = 0, \tag{2.6a}$$

where $\mathbf{u}$ and p are the local fluid velocity and pressure. The no-slip condition on the surfaces S of the micro-organism and S_B of any surrounding or nearby solid objects yields

$$\mathbf{u}_S = \mathbf{v}(s,t), \quad \mathbf{u}_{S_B} = \mathbf{v}_{S_B}, \tag{2.6b}$$

where $\mathbf{v}_{S_B}$ represents the local velocity on S_B. Here we have extended our definitions of $\mathbf{v}$ and s to include the head. The laws of conservation of linear and angular momentum for the organism require

$$\int_S (\boldsymbol{\sigma} - p\mathbf{I}).\mathbf{n}\,dS = 0, \tag{2.7}$$

$$\int_S \boldsymbol{\chi} \times (\boldsymbol{\sigma} - p\mathbf{I}).\mathbf{n}\,dS = 0, \tag{2.8}$$

respectively, where $\sigma_{ij} = \mu(\partial u_i/\partial x_j + \partial u_j/\partial x_i)$ is the viscous stress tensor. If we were now to specify the local contractility or beat of the flagellum, (2.1)–(2.8) would uniquely determine the motion $\mathbf{v}(s,t)$ of the organism. Rather than so doing, we shall, as discussed earlier, substitute two alternative conditions. First, we require that the rate of viscous working by the organism against the fluid be minimal at all times. This condition is equivalent to minimizing the global rate of instantaneous viscous dissipation in the fluid

$$\int_V \sigma_{ij}\sigma_{ij}\,dV.$$

As a second condition, we must make a general statement about the net motion of the organism. One possibility is to specify the velocity $\mathbf{v}_c$ of the centre of mass

$$\int_0^L \rho(s)\,\mathbf{v}(s,t)\,ds = \mathbf{v}_c \int_0^L \rho(s)\,ds, \tag{2.9}$$

where ρ is the density of the organism including the head. For a given initial position $\boldsymbol{\chi}_0(s)$, we then have the following system:

$$\partial\boldsymbol{\chi}/\partial t = \mathbf{v}(s,t), \quad \boldsymbol{\chi}(s,0) = \boldsymbol{\chi}_0(s), \tag{2.10}$$

where $\mathbf{v}$ is the instantaneous solution of†

$$\min_{\mathbf{v}} \left\{ \int_V \sigma_{ij}\sigma_{ij}\,dV \,\middle|\, \mu\nabla^2\mathbf{u} = \nabla p, \quad \nabla.\mathbf{u} = 0 \quad \text{in } V, \quad \mathbf{u}_S = \mathbf{v}, \quad \mathbf{u}_{S_B} = \mathbf{v}_{S_B}, \right.$$
$$\int_S (\boldsymbol{\sigma} - p\,\mathbf{I}).\mathbf{n}\,dS = 0, \quad \int_S \boldsymbol{\chi} \times (\boldsymbol{\sigma} - p\mathbf{I}).\mathbf{n}\,dS = 0,$$
$$\left. \frac{\partial v_l}{\partial s} = \frac{v_n}{R}, \quad \int_0^L \rho\mathbf{v}\,ds = \mathbf{v}_c \int_0^L \rho\,ds \right\}. \tag{2.11}$$

† The more general problem of optimal swimming from A to B, in which the total energy expended is minimized, would be

$$\min \int_0^T dt \int_V \sigma_{ij}\sigma_{ij}\,dV$$

subject to the same constraints as in (2.11). Optimal control problems of this nature have not been studied, the difficulty being that the moving boundaries (rather than velocities) are now the unknowns of the problem.

Equations (2.10) and (2.11) define an optimal control problem for a distributed parameter system in standard form, cf. Lions (1968). Use of the methods of optimal control theory in the solution of this problem places no restrictions on the size and shape of the head of the organism, the complexity of the flagellar undulations or on the presence of nearby solid boundaries, cf. § 3.

We now introduce several simplifications and define a modified optimal control problem, one for which analytical solution is possible. We employ resistive-force theory, introduced in § 1, to describe the hydrodynamics, and assume that the resistance coefficients are effectively constant. We confine the undulations of the flagellum to a single plane. Finally, we introduce an alternative specification of the forward swimming of the organism, viz.

$$\frac{1}{L}\int_0^L \mathbf{v}.\mathbf{l}\,ds \equiv v_k. \tag{2.12}$$

In replacing the vector swimming constraint (2.9) by the scalar constraint (2.12), we should like to specify the component of the swimming velocity in the direction of an effective body axis. Thus we might require

$$\langle \mathbf{l}\rangle.\frac{1}{L}\int_0^L \mathbf{v}\,ds \equiv v_{kk}, \tag{2.13}$$

where

$$\langle \mathbf{l}\rangle = \frac{1}{L}\int_0^L \mathbf{l}\,ds.$$

For flagellar undulations of small amplitude, (2.12) and (2.13) are effectively equivalent. Indeed, in this case one can easily show that

$$\mathbf{v}_c = [(\gamma-1)/\gamma]\langle \mathbf{l}\rangle v_k - C_H^* \mathbf{v}(0,t),$$

where $\gamma = C_N/C_L$ and $C_H^* = C_H/C_L$. However, it is difficult to provide a physical interpretation of (2.12) for more general undulations. This condition does require the organism to swim. Moreover, it enables us to formulate an analytical solution to the optimal control problem, which can now be posed as

$$\min_{v_l, v_n}\left\{C_L\int_0^L (v_l^2+\gamma v_n^2)\,ds + C_H v_H^2 + T_H\omega_H^2 \middle| C_L\int_0^L (v_l\mathbf{l}+\gamma v_n\mathbf{n})\,ds + C_H\mathbf{v}_H = 0,\right.$$
$$\left. C_L\int_0^L \boldsymbol{\chi}\times(v_l\mathbf{l}+\gamma v_n\mathbf{n})\,ds + T_H\boldsymbol{\omega}_H = 0,\quad \frac{1}{L}\int_0^L v_l\,ds = v_k,\quad \frac{\partial v_l}{\partial s} = \frac{v_n}{R}\right\}. \tag{2.14}$$

Here

$$\boldsymbol{\omega}_H = \mathbf{l}(0,t)\times\partial\mathbf{v}(0,t)/\partial s \quad \text{and} \quad \mathbf{v}_H = v(0,t).$$

The trajectory of the organism, represented by $\boldsymbol{\chi}(s,t)$, is obtained by integrating the partial differential equation

$$\left.\begin{aligned} &\partial\boldsymbol{\chi}(s,t)/\partial t = v_l(s,t)\,\mathbf{l}(s,t) + v_n(s,t)\,\mathbf{n}(s,t),\\ \text{with}\quad &\boldsymbol{\chi}(s,0) = \boldsymbol{\chi}_0(s),\quad (s,t)\in[0,L]\times[0,T],\end{aligned}\right\} \tag{2.15}$$

where $(v_l(s,t), v_n(s,t))$ is a solution of (2.14) at each time.

3. Solution of the problem for a headless organism

For a headless organism, $\mathbf{D}_H = \mathbf{M}_H = 0$. Problem (2.14) is then a standard optimal control problem with linear dynamics and quadratic cost. It can be solved by means of the maximum principle of Pontryagin *et al.* (1962). We can summarize the results by the following proposition.

Proposition 1. If the three integral constraints are physically compatible, then (2.14) has a unique solution (v_l, v_n). Furthermore,

$$v_l \mathbf{l} + v_n \mathbf{n} = \boldsymbol{\nu} + \boldsymbol{\omega} \times \boldsymbol{\chi} + \delta \mathbf{l}, \tag{3.1}$$

where $\boldsymbol{\nu} = (\nu_1, \nu_2, 0)$, $\boldsymbol{\omega} = (0, 0, \omega)$ and δ are independent of s and are determined by solving the 4×4 linear system

$$\int_0^L (v_l \mathbf{l} + \gamma v_n \mathbf{n})\, ds = 0, \quad \int_0^L \boldsymbol{\chi} \times (v_l \mathbf{l} + \gamma v_n \mathbf{n})\, ds = 0, \tag{3.2}$$

$$\frac{1}{L}\int_0^L v_l\, ds = v_k \tag{3.3}$$

with (v_l, v_n) given by (3.1).

Proof. Proposition 1 can be formally proved by use of the maximum principle. Here, however, we present an alternative proof which uses the methods of the calculus of variations, more familiar in traditional fluid dynamics. The equivalence of this approach and direct use of the maximum principle can be demonstrated.

Making use of the no-stretch condition, problem (2.14) becomes

$$\min\left\{\int_0^L (v_l^2 + \gamma R^2 v_l'^2)\, ds \,\middle|\, \int_0^L (v_l \mathbf{l} + \gamma R v_l' \mathbf{n})\, ds = 0, \quad \int_0^L \boldsymbol{\chi} \times (v_l \mathbf{l} + \gamma R v_l' \mathbf{n})\, ds = 0, \quad \frac{1}{L}\int_0^L v_l ds = v_k\right\}, \tag{3.4}$$

where $v_l' = \partial v_l / \partial s$. Therefore, by definition, (v_l, v_n) is optimum only if

$$\int_0^L (v_l \delta v_l + \gamma R^2 v_l' \delta v_l')\, ds \geqslant 0 \tag{3.5}$$

for all $\delta v_l(s)$ and $\delta v_l'(s)$ such that

$$\left.\begin{aligned} \int_0^L (\delta v_l \mathbf{l} + \gamma R \mathbf{n}\, \delta v_l')\, ds = 0, \quad \int_0^L \boldsymbol{\chi} \times (\delta v_l \mathbf{l} + \gamma R \mathbf{n}\, \delta v_l')\, ds = 0, \\ \int_0^L \delta v_l ds = 0. \end{aligned}\right\} \tag{3.6}$$

Here δv_l and $\delta v_l'$ represent small increments in v_l and v_l', respectively. Let $\boldsymbol{\nu}$, $\boldsymbol{\omega}$ and δ be Lagrange multipliers associated with the constraints. Then (3.5) and (3.6) are equivalent to

$$\int_0^L [v_l - \boldsymbol{\nu}.\mathbf{l} - \boldsymbol{\omega}.(\boldsymbol{\chi} \times \mathbf{l}) - \delta]\, \delta v_l ds + \int_0^L \gamma R[R v_l' - \boldsymbol{\nu}.\mathbf{n} - \boldsymbol{\omega}.(\boldsymbol{\chi} \times \mathbf{n})]\, \delta v_l' ds \geqslant 0 \tag{3.7}$$

for all δv_l and $\delta v_l'$. Integrating the second integral by parts, we obtain

$$-\int_0^L \gamma \frac{\partial}{\partial s}\{R[Rv_l' - \boldsymbol{\nu}.\mathbf{n} - (\boldsymbol{\omega}\times\boldsymbol{\chi}).\mathbf{n}]\}\,\delta v_l\,ds + \gamma R[Rv_l' - \boldsymbol{\nu}.\mathbf{n} - (\boldsymbol{\omega}\times\boldsymbol{\chi}).\mathbf{n}]\,\delta v_l|_{s=0}^{s=L}.$$

Define now $\mathbf{w} \equiv v_l\mathbf{l} + v_n\mathbf{n} - \boldsymbol{\nu} - \boldsymbol{\omega}\times\boldsymbol{\chi}$. Then, since $Rv_l' = v_n$, (3.7) becomes

$$\int_0^L \left[(w_l - \delta) - \gamma \frac{\partial}{\partial s}(w_n R)\right]\delta v_l\,ds + \gamma[R(L,t)\,w_n(L,t)\,\delta v_l(L,t) - R(0,t)\,w_n(0,t)\,\delta v_l(0,t)] \geqslant 0. \quad (3.8)$$

for all δv_l, where w_l and w_n are the $\mathbf{l}$ and $\mathbf{n}$ components of $\mathbf{w}$, respectively. $\mathbf{w}$ may be thought of as the velocity of deformation of the flagellum. Equation (3.8) implies that

$$\left.\begin{aligned} w_l - \gamma\,\partial(Rw_n)/\partial s &= \delta, \\ w_n(0,t) = w_n(L,t) &= 0. \end{aligned}\right\} \quad (3.9)$$

Making use of the no-stretch condition, we have

$$\partial w_l/\partial s = w_n/R. \quad (3.10)$$

Now differentiating (3.9) and using (3.10), we obtain

$$\left.\begin{aligned} \gamma\,\partial^2(Rw_n)/\partial s^2 &= w_n/R, \\ w_n(0,t) = w_n(L,t) &= 0. \end{aligned}\right\} \quad (3.11)$$

Equation (3.11) has the unique solution

$$w_n(s,t) \equiv 0 \quad \text{for all} \quad s\in[0,L].$$

Thence from (3.9), $w_l(s,t) = \delta$ for all s, and $v_l\mathbf{l} + v_n\mathbf{n} = \boldsymbol{\nu} + \boldsymbol{\omega}\times\boldsymbol{\chi} + \delta\mathbf{l}$. Q.E.D.

The undulations of a swimming flagellum can, of course, always be decomposed into a rigid-body translation and rotation and a velocity of deformation relative to the rigid-body movement. Equation (3.1) implies that the optimal deformation is a sliding of constant magnitude along the entire instantaneous axis of the flagellum. It is readily shown that

$$\dot{E} = C_L L v_k \delta. \quad (3.12)$$

Thus, since $\dot{E}$ is non-negative, $\operatorname{sgn}\delta = \operatorname{sgn} v_k$, i.e. the sliding is forward, in the direction of propulsion.

The deformation velocity $\delta(t)\,\mathbf{l}(s,t)$ is particularly simple to analyse. Let $\boldsymbol{\xi}(s,t)$ be the position vector of a point on the axis of the flagellum as measured in a co-ordinate frame translating with linear velocity $\boldsymbol{\nu}(t)$ and rotating with angular velocity $\boldsymbol{\omega}(t)$. Then, since

$$\mathbf{l}(s,t) = (\partial\boldsymbol{\xi}(s,t)/\partial s)/\|\partial\boldsymbol{\xi}/\partial s\| \quad \text{and} \quad \mathbf{w}(s,t) = \partial\boldsymbol{\xi}(s,t)/\partial t$$

we have

$$\left.\begin{aligned} \partial\boldsymbol{\xi}(s,t)/\partial t &= \delta(t)\,\partial\boldsymbol{\xi}(s,t)/\partial s, \\ \boldsymbol{\xi}(s,0) &= \boldsymbol{\xi}_0(s), \quad s\in[0,L], \quad t\in[0,T]. \end{aligned}\right\} \quad (3.13)$$

Letting $\tilde{\boldsymbol{\xi}}_0(s)$, $s\in[-\infty,\infty]$, be any piecewise differentiable extension of $\boldsymbol{\xi}_0(s)$, the general solution of (3.13) is

$$\boldsymbol{\xi}(s,t) = \tilde{\boldsymbol{\xi}}_0\left(s + \int_0^t \delta(\zeta)\,d\zeta\right). \quad (3.14)$$

Thence the optimal swimming is completely described, in the original fixed frame of reference, by $\boldsymbol{\chi}(s,t) = (\chi_1(s,t), \chi_2(s,t))$, where

$$\chi_1 + i\chi_2 = \exp\left[i\int_0^t \omega(\zeta)\,d\zeta\right]\left\{\tilde{\xi}_{01}\left(s+\int_0^t \delta(\zeta)\,d\zeta\right) + i\tilde{\xi}_{02}\left(s+\int_0^t \delta(\zeta)\,d\zeta\right)\right.$$
$$\left. + \int_0^t [\nu_1(\zeta) + i\nu_2(\zeta)]\exp\left[-i\int_0^\zeta \omega(\hat{\zeta})\,d\hat{\zeta}\right]d\zeta\right\}. \quad (3.15)$$

Noting that $\boldsymbol{\omega}$ must lie normal to the plane of $\boldsymbol{\nu}$, we have introduced complex notation for compactness here, and have assumed that the fixed and moving co-ordinate frames coincide at $t = 0$. Notably (3.15) indicates that the solution to the general problem, cf. (2.14) and (2.15), is not unique. There exist an infinite number of solutions, each completely determined by a given infinite differentiable curve $\tilde{\boldsymbol{\xi}}_0(s)$, $s \in [-\infty, \infty]$, which coincides with $\boldsymbol{\xi}_0(s)$ for $s \in [0, L]$. The position of the flagellum at time t is obtained from $\boldsymbol{\xi}_0$ by sliding along $\tilde{\boldsymbol{\xi}}_0$ a distance

$$\int_0^t \delta(\zeta)\,d\zeta,$$

translating a distance

$$\int_0^t \boldsymbol{\nu}(\zeta)\exp\left[-i\int_0^\zeta \omega(\hat{\zeta})\,d\hat{\zeta}\right]d\zeta$$

and rotating through an angle

$$\int_0^t \omega(\zeta)\,d\zeta,$$

where $\{\nu_1, \nu_2, \omega, \delta\}$ is the solution at each time of (3.3).

It is also noteworthy that there exist compatibility conditions between the specification of the initial shape $\boldsymbol{\xi}_0(s)$ and the requirement that the flagellum swim optimally. For example, suppose that $\boldsymbol{\xi}_0$ is a portion of a circle of radius R and $\tilde{\boldsymbol{\xi}}_0$ is chosen as the whole circle. From (3.1), then, $\mathbf{v}(s,t) = \boldsymbol{\nu}(t) + (\delta - R\omega)\mathbf{l}$. In this case, the linear system (3.2) and (3.3) has no solution, there being three unknowns and four independent equations. That is, forward swimming is impossible, and there is no analytical solution to (3.2) and (3.3). If, say, $\boldsymbol{\xi}_0$ is a portion of a parabola and $\tilde{\boldsymbol{\xi}}_0$ is the entire parabola, there exists the possibility that $\delta(t) \to \infty$ for $t \to t_0$. Here, also, the linear system has no solution at $t = t_0$. Therefore an acceptable extension of $\boldsymbol{\xi}_0$, one that is capable of perpetuating the swimming, must have no infinite branch on which the radius of curvature tends to a constant, and no points at which the linear system (3.2) and (3.3) is singular. An obvious possibility is a curve that is, at least in some approximate sense, periodic. In this case, we may regard the optimal deformation as backward propagation of travelling waves which, for a periodic curve, have phase speed $-c(t)$, where the time-average values $\bar{c}$ and $\bar{\delta}$ are related via

$$\bar{c} = \bar{\delta}\frac{1}{L}\int_0^L l_1(s,t)\,ds, \quad (3.16)$$

l_1 being the component of $\mathbf{l}$ along the instantaneous curve axis. The angular velocity $\boldsymbol{\omega}(t)$ is then a pitching motion about a mean position.

In optimal control theory (3.9) and (3.10) are referred to as the optimality conditions of the problem given by (2.14). They are a direct consequence of the hypothesis of a minimum rate of working. Together with $\boldsymbol{\xi}_0(s)$ they can be used to describe the distribution of internal bending movements $\mathbf{M}_{\text{int}}(s,t)$ required of the flagellar contraction mechanism for the swimming to be optimal. In general

$$\mathbf{M}_{\text{int}}(s,t) = \mathbf{M}_{\text{int}}(0,t) + C_L \int_0^s [\boldsymbol{\xi}(s,t) - \boldsymbol{\xi}(s',t)] \times [\mathbf{v}_l(s',t) + \gamma \mathbf{v}_n(s',t)]\, ds', \quad (3.17)$$

while, in linearized theory, the approximation

$$\partial^2 \mathbf{M}_{\text{int}} / \partial s^2 \doteq C_N \mathbf{v}_n(s,t) \quad (3.18)$$

is made. Since here $\mathbf{v}(s,t) = \boldsymbol{\nu}(t) + \boldsymbol{\omega}(t) \times \boldsymbol{\xi}(s,t) + \delta(t)\,\mathbf{l}(s,t)$, (3.17) and (3.18) are notable in that they imply a particular relation between $\mathbf{M}_{\text{int}}$ and the radius of curvature R, an important parameter in studies of the contraction mechanism.

4. Some extensions of the results

Influence of the head

Since the drag $\mathbf{D}_H$ and the moment $\mathbf{M}_H$ acting on the head of an organism are functions of the velocity and its s derivative at that end of the flagellum, the optimality conditions, cf. (3.9) and (3.10), must be modified. In order to compare the relative importance of $\mathbf{D}_H$ and $\mathbf{M}_H$, we non-dimensionalize (3.2) and (3.3), taking v_k as a characteristic speed and introducing Λ as a length characteristic of changes along the flagellum. For example, Λ would be the wavelength as measured along the flagellum for a periodic curve. If a caret denotes a dimensionless variable, (3.2) and (3.3) can be written as

$$\hat{\mathbf{L}}_1(\hat{\mathbf{v}}) = (a/\Lambda)\, \hat{\mathbf{v}}(0,t), \quad (4.1)$$

$$\hat{\mathbf{L}}_2(\hat{\mathbf{v}}) = (a/\Lambda)^3 \mathbf{1}(0,\hat{t}) \times \partial \hat{\mathbf{v}}(0,\hat{t}) / \partial \hat{s}, \quad (4.2)$$

where the dimensionless operators $\hat{\mathbf{L}}_1$ and $\hat{\mathbf{L}}_2$, of equal order of magnitude, symbolize respectively the force and moment generated by the flagellum. Typically $a/\Lambda \ll 1$; for example, the values $a = 3\,\mu$m and $\Lambda = 25\,\mu$m are characteristic of bull spermatozoa. Thence, a reasonable first approximation is to consider the effect of head drag while neglecting the influence of the head-induced moment.† In this case, (3.10) and (3.11) remain the same, but the boundary conditions are altered, viz.

$$\left.\begin{aligned} w_l - \gamma\, \partial(R w_n)/\partial s = \delta, \quad \partial w_l/\partial s = w_n/R, \\ w_n(0,t) = [C_H^*/R(0,t)]\,[w_l(0,t) - \delta], \quad w_n(L,t) = 0. \end{aligned}\right\} \quad (4.3)$$

Here the coupling of the optimality conditions to the dynamics of the motion precludes general analytic determination of the nature of the deformation velocity $\boldsymbol{\omega}$. An instructive exception, however, is the case where the initial curve $\boldsymbol{\xi}_0(s)$ is periodic and comprised of arcs of circles of equal radius, so that

† Such an approximation is primarily applicable to the case of two-dimensional undulations, and would not necessarily be appropriate for, say, a spiral beat.

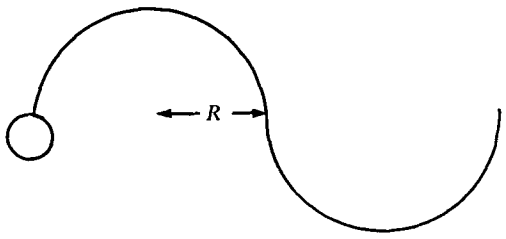

FIGURE 2. A flagellar wave form comprised of arcs of circles.

R is constant, see figure 2. In this case we can solve (4.3) analytically, and thus gain some insight into the onset of optimal swimming. We obtain

$$w_l(s,t) = \delta\left\{1-\cosh\left(\frac{L-s}{\gamma^{\frac{1}{2}}R}\right)\left[\frac{\gamma^{\frac{1}{2}}C_H^*/R\sinh(L/\gamma^{\frac{1}{2}}R)}{1+\gamma^{\frac{1}{2}}C_H^*/R\sinh(L/\gamma^{\frac{1}{2}}R)}\right]\right\}, \tag{4.4}$$

$$w_n(s,t) = -\delta\sinh\left(\frac{L-s}{\gamma^{\frac{1}{2}}R}\right)\left[\frac{C_H^*/R\sinh(L/\gamma^{\frac{1}{2}}R)}{1+\gamma^{\frac{1}{2}}C_H^*/R\sinh(L/\gamma^{\frac{1}{2}}R)}\right]. \tag{4.5}$$

The initial deformation indicated by (4.4) and (4.5) tends to increase the wave amplitude and decrease the wavelength exponentially as the wave propagates away from the head. The deformation is therefore no longer a simple sliding. Notably, the tendency of the head of the organism to twitch is diminished. Such an exponentially growing wave envelope is characteristic of many mammalian spermatozoa.

Three-dimensional motions without a head

If the flagellum is moving in an effectively infinite fluid, the analysis of §3 can be readily extended to include three-dimensional undulations. The requirement of an infinite fluid is due to the notion that, in such a case, the resistance coefficient characterizing the binormal component of the undulations is identical to the normal coefficient C_N. Here $\mathbf{v} = v_l\mathbf{l}+v_n\mathbf{n}+v_b\mathbf{b}$, where $\mathbf{b}(s,t)$ is the unit binormal. The no-stretch condition (2.5) remains the same provided that $\mathbf{n}$ is the principal normal. Thence (3.4) becomes

$$\min\left\{\int_0^L [v_l^2+\gamma(v_n^2+v_b^2)]\,ds \,\middle|\, \frac{\partial v_l}{\partial s} = \frac{v_n}{R}, \quad \int_0^L [v_k\mathbf{l}+\gamma(v_n\mathbf{n}+v_b\mathbf{b})]\,ds = 0,\right.$$
$$\left.\int_0^L \boldsymbol{\chi}\times[v_k\mathbf{l}+\gamma(v_n\mathbf{n}+v_b\mathbf{b})]\,ds = 0, \quad \frac{1}{L}\int_0^L v_l\,ds = v_k\right\}. \tag{4.6}$$

In this case it can again be demonstrated that $\mathbf{v} = \boldsymbol{\nu}(t)+\boldsymbol{\omega}(t)\times\boldsymbol{\chi}+\delta(t)\,\mathbf{l}$ although $\boldsymbol{\nu}$ and $\boldsymbol{\omega}$ are now full three-dimensional vectors. The suggestions in the remainder of §3 may also be shown to apply. Notably, we have in (4.6) excluded the influence of flagellar rotations about the local axis $\mathbf{l}$ on conservation of angular momentum. Such rotations, of magnitude Ω_s, say, give rise to a torque per unit length of magnitude $4\pi\mu r_0^2\Omega_s$. This 'rotlet' effect may be significant for undulations of small amplitude. However, its presence does not alter the conclusions

here. Indeed, using the rotlet effect it is possible to derive optimality criteria on the production of intrinsic flagellar spin, for organisms with or without heads. We shall present such a study in a succeeding publication.

5. Propagation of periodic waves

The analysis of the preceding sections has provided some qualitative insight into the nature of optimal swimming. In the remainder of the paper we shall examine some examples of specific wave forms, in order to gain some quantitative insight into these suggestions. The scalar swimming requirement used earlier does not constrain an organism to proceed along any particular trajectory. Since a periodic beat is allowable, and often observed; and since such a beat, if symmetrical, will tend to propel an organism along a straight line in the mean, it is instructive to consider examples of such cases.† The object is then to determine the relative importance of the propagated wave speed or beat frequency, wave shape and the number of wavelengths, and where possible to optimize with respect to these parameters. Rather than specifying the shape $\boldsymbol{\xi}_0(s)$, $s \in [0, L]$, and speed v_k and then solving a 4×4 system for ν_1, ν_2, ω and δ, we shall pose an equivalent problem in which we specify $\boldsymbol{\xi}_0$ and δ. The rigid-body propulsive movements ν_1, ν_2, and ω are then obtainable from the equations of motion alone, a 3×3 system, after which v_k can be calculated. We shall work in a moving co-ordinate system whose x axis coincides with the mean axis of the periodic curve $\boldsymbol{\xi}_0(s)$, and whose origin is the mean position of the forward end of the flagellum. Viewed in this system, the flagellar undulations consist of a forward longitudinal sliding with velocity $-\delta \mathbf{l}$ and a backward rigid-body translation with velocity $c\mathbf{e}_x$, δ and c being related via (3.16). Thus, the co-ordinate system translates with velocity $\mathbf{v} - c\mathbf{e}_x \equiv -\mathbf{V}_p$ and rotates with angular velocity $\omega \mathbf{e}_z$, viz.

$$\left.\begin{aligned} \mathbf{v}(s,t) &= -\mathbf{V}_p(t) + \boldsymbol{\omega}(t) \times \boldsymbol{\xi}(s,t) + \partial \boldsymbol{\xi}(s,t)/\partial t, \\ \partial \boldsymbol{\xi}/\partial t &= c\mathbf{e}_x - \delta \mathbf{l}, \end{aligned}\right\} \tag{5.1}$$

with $\boldsymbol{\xi} = x\mathbf{e}_x + y\mathbf{e}_y$. $-\mathbf{V}_p$ may be thought of as the propulsive velocity of the organism relative to the moving co-ordinate axes, the minus sign being introduced so that V_p is inherently positive. Since the shape of the curve is periodic, the functions $x(s)$ and $y(s)$ are such that

$$x(s+\Lambda) = x(s) + \lambda, \quad y(s+\Lambda) = y(s), \tag{5.2}$$

where Λ is a wavelength measured along the flagellum and $\lambda = (c/\delta)\Lambda$ is a wavelength measured along the x axis. We shall assume that the curve contains an integral number n of wavelengths. Since the undulations are travelling waves,

$$\boldsymbol{\xi}(s,t) = \boldsymbol{\xi}_0\left[s - \int_0^t \delta(\zeta)\, d\zeta\right]. \tag{5.3}$$

† Apart from externally induced tactic responses (rheotaxis, chemotaxis, etc.) it is the tendency of many normal mature spermatozoa to swim along trajectories whose radius of curvature is large compared with the organism length.

We may define

$$\mathbf{l} = \sin\alpha\mathbf{e}_x + \cos\alpha\mathbf{e}_y, \quad \mathbf{n} = -\cos\alpha\mathbf{e}_x + \sin\alpha\mathbf{e}_y, \tag{5.4}$$

where

$$dx/ds = \cos\alpha, \quad dy/ds = \sin\alpha. \tag{5.5}$$

Substituting (5.1) and (5.4) into the equations of motion for the flagellum, and noting that certain terms vanish owing to the symmetry of the curve, we obtain the following system of equations:

$$V_{px}\left[C_{Hx} + \frac{\gamma}{\gamma-1}L - \int_0^L \cos^2\alpha\, ds\right] + \omega\left[\int_0^L x\sin\alpha\cos\alpha\, ds\right]$$
$$= c\left[L - \int_0^L \cos^2\alpha\, ds\right] + \frac{C_H^*}{\gamma-1}[c - \delta\cos\alpha(0,t)], \tag{5.6}$$

$$V_{py}\left[C_{Hy} + \frac{1}{\gamma-1}L + \int_0^L \cos^2\alpha\, ds\right]$$
$$-\omega\left[\frac{1}{\gamma-1}\int_0^L x\, ds + \int_0^L x\cos^2\alpha\, ds\right] = -\frac{C_H^*}{\gamma-1}\delta\sin\alpha(0,t), \tag{5.7}$$

$$V_{px}\left[-\int_0^L x\sin\alpha\cos\alpha\, ds\right] + V_{py}\left[\frac{1}{\gamma-1}\int_0^L x\, ds + \int_0^L x\cos^2\alpha\, ds\right]$$
$$+\omega\left[-T_H^* - \frac{\gamma}{\gamma-1}\int_0^L (x^2+y^2)\, ds + \int_0^L (x\sin\alpha - y\cos\alpha)^2\, ds\right]$$
$$= c\left[-\int_0^L x\sin\alpha\cos\alpha\, ds\right] + \delta\left[\frac{T_H^*}{R(0,t)} - \int_0^L x\sin\alpha\, ds\right]. \tag{5.8}$$

Here $T_H^* = T_H/C_L$. Upon determination of V_{px}, V_{py} and ω, the absolute propulsive velocity relative to the fixed (X, Y) is then

$$V_{pX} = V_{px}\cos\theta - V_{py}\sin\theta, \tag{5.9}$$

$$V_{pY} = V_{px}\sin\theta + V_{py}\cos\theta, \tag{5.10}$$

where

$$\theta(t) = \theta(0) + \int_0^t \omega(\zeta)\, d\zeta. \tag{5.11}$$

Equations (5.6)–(5.8) are analogous to the system introduced by Brokaw (1972), and also used by Shack, Fray & Lardner (1971), working in a co-ordinate system moving with the forward end of the flagellum. If head effects are neglected, viz. $C_H = T_H = 0$, then $V_{py} \to 0$ and $\omega \to 0$ as the number of wavelengths increases. The problem thus reduces to the case of unidirectional swimming, originally considered by Gray & Hancock (1955) and recently treated generally, along lines similar to these, by Lighthill (1974). The presence of a head will tend to damp the pitching motion ω. If in that case this motion is neglected, n being taken sufficiently large that angular momentum is automatically conserved, then V_{px} will contain an oscillatory, time-dependent component in addition to the constant term, which is now reduced owing to the drag of the head. Moreover, V_{py} will no longer vanish, but be an oscillatory function of time. In the mean, these time-dependent components of V_{px} and V_{py} may be expected to vanish, and thus not influence the effective swimming speed. Their significance lies in their effect

upon the rate of working by the organism, which depends upon the squares of velocities.

We seek analytical solutions of (5.6)–(5.8) for particular curve shapes. In order to examine the effect of pitching, we shall consider first a headless flagellum. One case for which analytical solution is possible is the traditional small amplitude sinusoid. Let $y(s,t) = b\sin k[x(s,t)-ct]$, where $bk \ll 1$. Then, since $\tan\alpha = dy/dx$,

$$\sin\alpha = bk\cos k[x(s,t)-ct]+O(bk)^3, \tag{5.12}$$

$$\cos\alpha = 1-\tfrac{1}{2}(bk)^2\cos^2 k[x(s,t)-ct]+O(bk)^4, \tag{5.13}$$

$$ds = dx[1+O(bk)^2], \tag{5.14}$$

$$\lambda/\Lambda = c/\delta = 1-\tfrac{1}{4}(bk)^2+O(bk)^4, \tag{5.15}$$

$$L = (2\pi n/k)\,[1+O(bk)^2]. \tag{5.16}$$

We can conveniently perform all integrations with respect to $x\in[x_0, n\lambda+x_0]$, where

$$kx_0 = kx(0,t) = -\tfrac{1}{4}(bk)^2\sin 2kct+O(bk)^4. \tag{5.17}$$

Substituting in (5.6)–(5.11) and retaining terms up to $O((bk)^2)$ we then obtain

$$V_{pX} = (bk)^2 c\left\{\frac{\gamma-1}{2}\left[1-\frac{3}{(\pi n)^2}\right]+\cos kct-\frac{3}{\pi n}\sin kct \right.$$
$$\left. -\left[\frac{3(3-\gamma)}{(2\pi n)^2}+\tfrac{1}{4}\right]\cos 2kct+\frac{9}{2(\pi n)^3}\sin 2kct\right\}, \tag{5.18}$$

$$V_{pY} = -(bk)\,c\,[\cos kct-(3/\pi n)\sin kct], \tag{5.19}$$

$$\omega = -3ck(bk)^2\sin kct/(\pi n)^2 \tag{5.20}$$

correct to $O((bk)^2)$. The time-average propulsive velocity is thus

$$\bar{\mathbf{V}}_p = \tfrac{1}{2}c(\gamma-1)\,(bk)^2\,[1-3/(\pi n)^2]\,(-\mathbf{e}_X). \tag{5.21}$$

The propulsive velocity for $\gamma = 2$ was considered by Shack *et al.* (1971).

Substituting in (2.12) and (3.12), it follows that

$$v_k = \frac{\gamma}{\gamma-1}v_c = \frac{\gamma}{\gamma-1}\bar{V}_p, \tag{5.22}$$

$$\bar{E} = LC_N c^2(bk)^2[1-3/(\pi n)^2]. \tag{5.23}$$

When interpreting (5.21) and (5.23), it must be remembered that the resistance coefficients do depend, albeit logarithmically, upon the wavelength. The original values suggested by Gray & Hanock (1955) were approximations obtained heuristically from Hancock's (1953) analysis. Shack *et al.* applied Cox's (1970) method to an undulating slender body, using conservation of linear momentum only. For sinusoidal motions of small amplitude, they obtained explicit expressions for C_N and C_L, with errors $O[\ln^{-2}(kr_0)]$. Recently Lighthill (1974) has obtained similar values to those of Shack *et al.* via an alternative, semi-heuristic method. Lighthill's analysis yields an identical value of C_N and a slightly larger C_L, hence a slightly lower γ. Since this latter approach suggests applicability to more general periodic wave forms, we shall use its results here.

For purposes of optimization, the distinction is insignificant. However, the limit of extendibility to wave forms of large amplitude is not clear (see § 6).

Lighthill's results can be written as

$$C_L = -2\pi\mu/(\ln(kr_0) + 0{\cdot}384), \tag{5.24}$$

$$C_N = -4\pi\mu/(\ln(kr_0) - 0{\cdot}616), \tag{5.25}$$

where r_0 is the radius of the flagellum. For the small amplitude sinusoid,

$$\ln(kr_0) \doteqdot \ln n + \ln(2\pi r_0/L) \tag{5.26}$$

correct to $O(bk)$. Typically, we might take $r_0 = 0{\cdot}4\,\mu$m and $L = 60\,\mu$m, so that here

$$C_L = -2\pi\mu/(\ln n - 2{\cdot}834), \tag{5.27}$$

$$C_N = -4\pi\mu/(\ln n - 3{\cdot}834). \tag{5.28}$$

Now the restriction $bk \ll 1$ precludes a meaningful investigation of the effect of wave amplitude upon optimal swimming. We shall, therefore, require that this parameter remain fixed, and thus restrict our investigation here to the effect of the number of wavelengths. It is then particularly interesting to note that, if account is taken of the variation of C_L and C_N with n, cf. (5.27) and (5.28), the values of $\overline{V}_p$ for $n = 1$ and $n = 2$ are virtually identical, the latter being very slightly higher. That is, the effect of the reduced γ for $n = 2$ is countered by the reduction in $\overline{V}_p$ for $n = 1$ due to pitching. For $n > 2$, pitching effectively ceases and further reduction in γ causes $\overline{V}_p$ to decrease. Combining (5.21) and (5.23), we have

$$\overline{\dot{E}} = \frac{L\overline{V}_p^2}{(bk)^2}\frac{C_N}{(\gamma-1)^2}\frac{(\pi n)^2}{(\pi n)^2 - 3}. \tag{5.29}$$

It follows that, for fixed $\overline{V}_p$ and bk, $\overline{\dot{E}}$ is an increasing function of n, although if the dependence of γ upon n were neglected, $\overline{\dot{E}}$ would decrease with increasing n. For the small amplitude sinusoid then, the smallest allowable number of wavelengths, $n = 1$, is preferable.

6. Two-dimensional propulsion by sawtooth waves

The results of § 5 for a small amplitude sinusoid are instructive, because they take a simple analytic form, and because of the assuredness with which the expressions for the resistance coefficients, cf. (5.24) and (5.25), are applied. The result that the reduction in γ with increasing n more than offsets the opposite effect of diminished pitching is of particular note. We should like, however, to obtain results for waves of finite amplitude, since they enable us to examine the trade-off between the number of wavelengths and wave amplitude.

A non-pitching, effectively headless flagellum, propagating the two-dimensional periodic waves introduced previously, expends hydrodynamic work at the rate†

$$\dot{E} = c^2 L C_L\left[\frac{1}{A^2} + \frac{1}{(\gamma-1)B - \gamma}\right], \tag{6.1}$$

† The presence of a head on a non-pitching flagellum does not alter this argument, and has been omitted here for the sake of algebraic clarity.

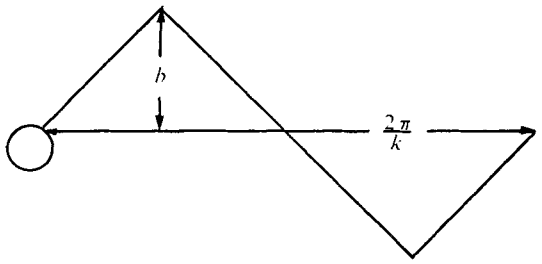

FIGURE 3. A flagellar wave form shaped like a sawtooth.

where $$A \equiv \frac{1}{L}\int_0^L \cos\alpha\, ds, \quad B \equiv \frac{1}{L}\int_0^L \cos^2\alpha\, ds. \tag{6.2}$$

Lighthill (1974) has noted that if $\dot{E}$ is regarded as a function of A and B, then the minimum is achieved when $A^2 = B =$ constant. Such a curve, for which $\cos\alpha$ is constant, is in the present context a symmetrical sawtooth; see figure 3. Since the propulsive velocity depends only upon B, this shape may be regarded as hydrodynamically optimal for non-pitching propulsion, and the tendency towards it noted in real flagellar wave forms. Moreover, the sawtooth is a shape for which (5.6)–(5.8) can be solved without numerical integration for waves of finite amplitude.

We shall represent a sawtooth of amplitude b and wavelength $2\pi/k$ by the expression $y = bf(kx)$, where, of course, an explicit Fourier series can be written down. The curve contains n wavelengths and propagates waves with phase speed c, the displacements of all points on the curve being in the $\pm y$ direction. The no-stretch condition can be written as [cf. (5.16)]

$$L = \frac{2\pi n}{k}\left[1 + \left(\frac{bk}{\frac{1}{2}\pi}\right)^2\right]^{\frac{1}{2}} \tag{6.3}$$

and

$$A = 2\pi n/kL. \tag{6.4}$$

It follows that the solution to (5.6)–(5.8) can be expressed as

$$\frac{V_{px}}{c} = \frac{F_2 + G_2 f^2(\tau)}{F_1 + G_1 f^2(\tau)}, \quad \frac{V_{py}}{c} = \frac{G_3 f(\tau)}{F_1 + G_1 f^2(\tau)}, \quad \frac{wL}{c} = \frac{G_4 f(\tau)}{F_1 + G_1 f^2(\tau)}, \tag{6.5), (6.6)}$$

(6.7)

where $\tau = 2kct/\pi$, and F_1, G_1, F_2, G_2, G_3 and G_4 are functions of γ, bk and n, and are given in the appendix. Note that the dimensionless unit sawtooth $f(\tau)$ has period 4. In order to determine the behaviour of $\theta(\tau)$ and evaluate the time averages of interest, it is necessary to consider only $\tau \in [0, 1]$ for which $f(\tau) = \tau$. It follows that the amplitude of the pitching $\theta_A \equiv \theta(1)$ is given by

$$\theta_A = \left|\frac{G_4}{2G_1}\ln\left(1 + \frac{G_1}{F_1}\right)\right|, \tag{6.8}$$

where we have taken $\theta(0) = 0$. Equation (6.8) is plotted in figure 4. Notably, regardless of whether or not account is taken of the variation of γ with wavelength (to be discussed shortly), in general $\theta_A \ll 1$, the pitching decreasing with

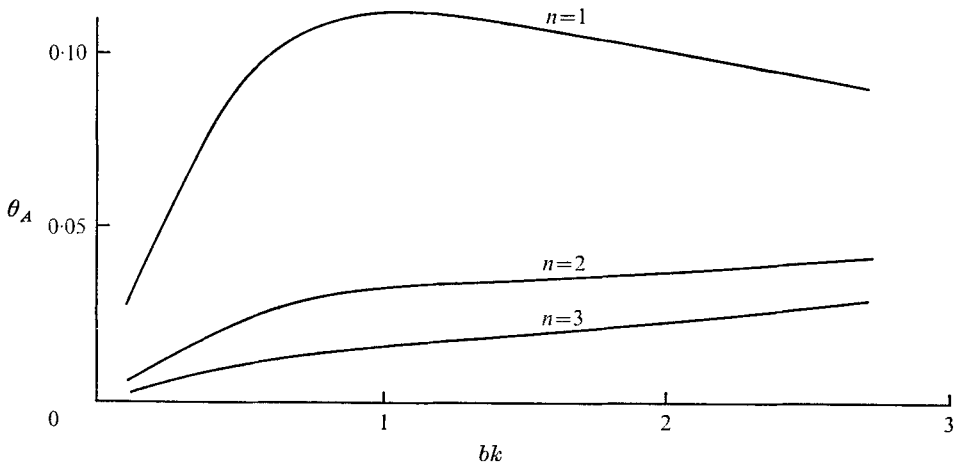

FIGURE 4. Variation of the pitching amplitude θ_A for a sawtooth beat. n is the number of wavelengths, b the amplitude and $2\pi/k$ the wavelength. The resistance coefficients vary and $r_0/L = 0{\cdot}0067$.

increasing n. It follows, just as in the example of a small amplitude sinusoid, that we may make the approximation $V_{pX} \doteqdot V_{px} - \theta V_{py}$ to reasonable accuracy. Thence taking the time average, i.e. integrating with respect to τ on $[0, 1]$, we obtain

$$\left.\begin{aligned} \frac{\overline{V}_{pX}}{c} &= \frac{G_2}{G_1} + \left(\frac{F_2}{F_1} - \frac{G_2}{G_1}\right) I - \frac{G_3 G_4}{8 G_1^2} \ln^2\left(1 + \frac{G_1}{F_1}\right), \\ \frac{\overline{V}_{py}}{c} &= 0, \end{aligned}\right\} \tag{6.9}$$

where

$$I = \frac{1}{2}\left|\frac{F_1}{G_1}\right|^{\frac{1}{2}} \ln\left[\frac{1 + |F_1/G_1|^{\frac{1}{2}}}{1 - |F_1/G_1|^{\frac{1}{2}}}\right]. \tag{6.10}$$

The time-averaged rate of working can be written as

$$\overline{E} = c^2 L C_L \left\{\frac{1}{A^2} - 1 + \frac{G_2}{G_1} + \left(\frac{F_2}{F_1} - \frac{G_2}{G_1}\right) I + \frac{G_5}{G_1}(1 - I)\right\}, \tag{6.11}$$

the final term being the direct contribution of the pitching motions.

Now in order to consider the behaviour of (6.9) and (6.10) account should be taken of the variation of C_L and C_N with wave shape. Lighthill's (1974) analysis has suggested that (5.24) and (5.25) are likely to be generally applicable to periodic waves. However, this applicability is limited to some extent, since for waves of sufficiently large amplitude the wave crests will be closely bunched, and the so-called 'neighbouring effect' (see Chwang & Wu 1971) will become important. Physically this means that the forces acting on an element ds of a particular wave are influenced by the presence of elements of neighbouring waves. Equations (5.24) and (5.25) indicate that γ decreases with decreasing wavelength while C_L and C_N both increase; see figures 5 and 6. However, the neighbouring effect is likely to increase C_N more than C_L; hence the reduction in γ will tend to be countered. Chwang & Wu have suggested that for $bk \lesssim 2$ the neighbouring effect may

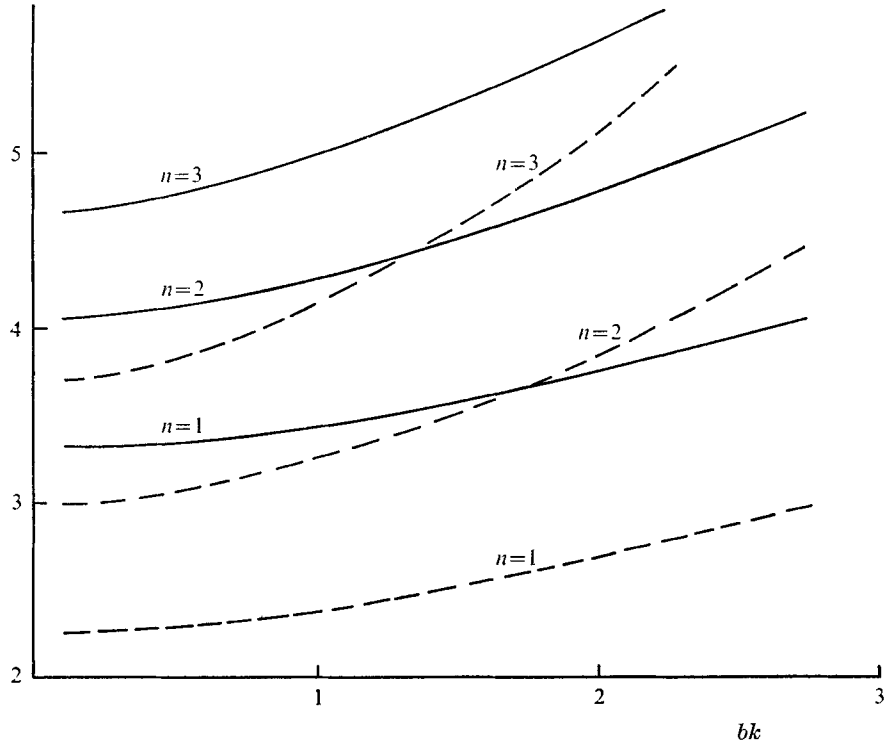

FIGURE 5. Dependence of the resistance coefficients upon the wave parameter of a sawtooth beat. $r_0/L = 0{\cdot}0067$. – – –, C_L/μ; ——, C_N/μ.

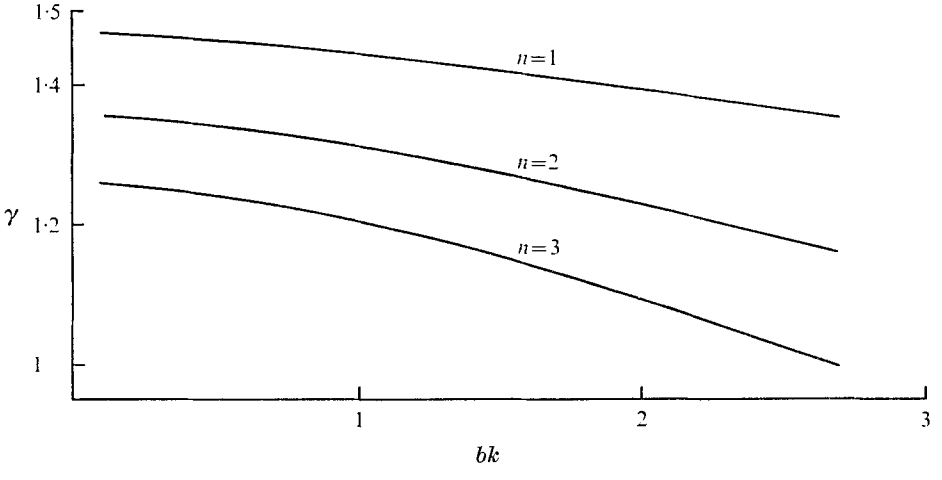

FIGURE 6. Variation of $\gamma = C_N/C_L$ for the sawtooth beat.

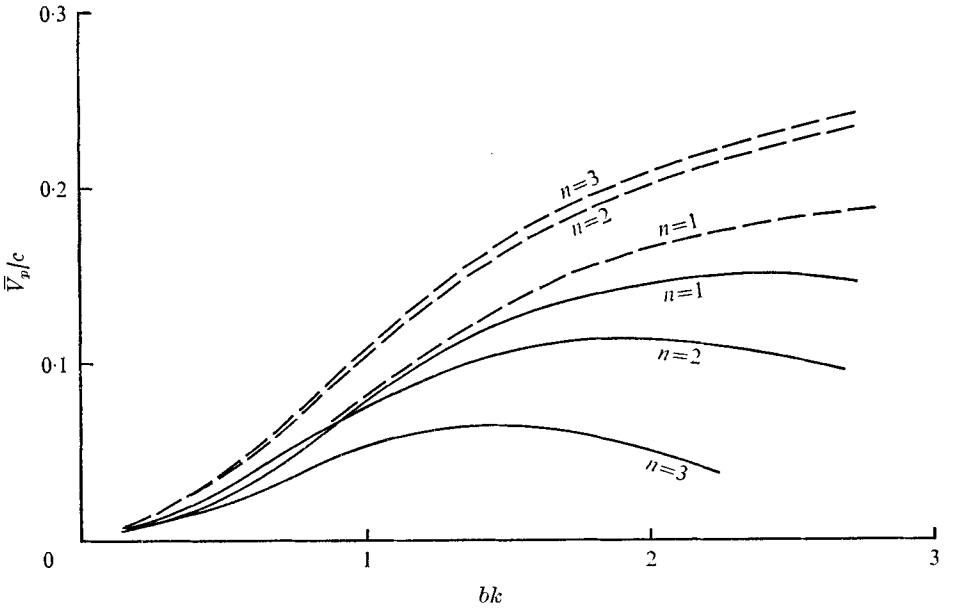

FIGURE 7. Time-average swimming speed for the sawtooth waves without a head. ——, γ varying with wavelength; – – –, γ fixed, $\gamma = 1{\cdot}471$, corresponding to $bk = n = 1$.

be negligible, a conclusion also implied in the work of Hancock (1953). In the present context we must remember, also, that increases in n for fixed b, as well as increases in b for fixed n, will diminish the wavelength, cf. (6.3), the former giving rise to a 'thickening effect' of the same consequence. Moreover, the onset of the neighbouring effect will be accentuated by the apparent thickening of the flagellum as n increases.

Bearing in mind that such a limitation on wave amplitude does exist, it is therefore instructive to consider the behaviour of (6.9) and (6.10) both allowing C_N and C_L to vary according to (5.24) and (5.25), and holding them constant at suitable average values. Figures 7 and 8 display the results. Note the fundamental difference between these two cases: variation of the resistance coefficients causes a single wavelength to yield a generally higher propulsive speed and a lower rate of working than two or more wavelengths; the opposite conclusion is reached if the resistance coefficients are held constant. We now seek to optimize the parameters n, b and k, i.e. fix $\overline{V}_{pX}$ and minimize $\overline{E}$. Equations (6.9) and (6.11) may be written symbolically as

$$V = c\mathscr{V}(bk, n), \quad E = \mu L c^2 \mathscr{E}(bk, n), \qquad (6.12), (6.13)$$

where we have dropped the overbars and also the subscript on V_{pX}. Since V is fixed, (6.13) can be expressed in dimensionless form as

$$\eta^{-1} \equiv E/\mu L V^2 = \mathscr{E}(bk, n)/\mathscr{V}^2(bk, n). \qquad (6.14)$$

η may be regarded as a propulsive efficiency whose maximum is sought. Note, however, that this is a purely mathematical definition, quantitative values of

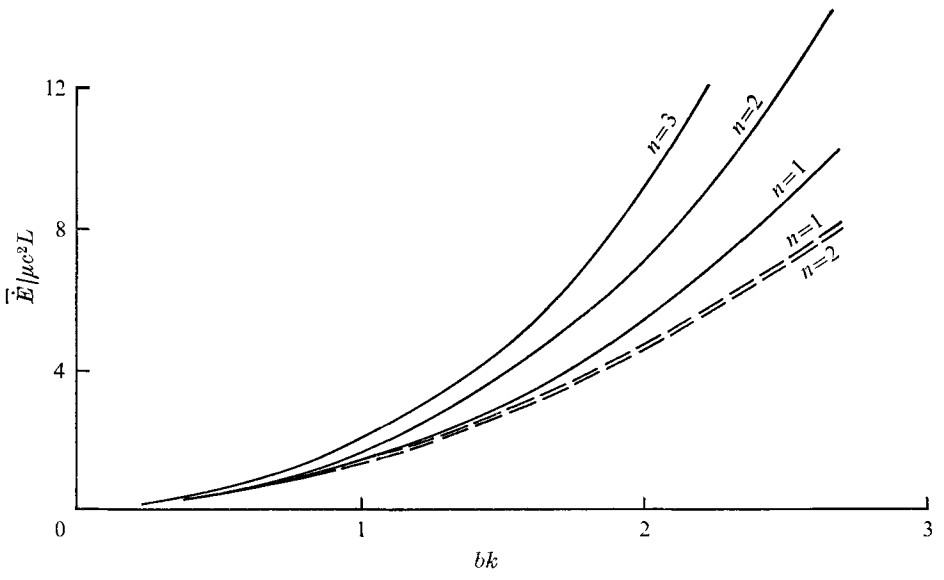

FIGURE 8. Time-average rate of working for the sawtooth waves without a head. ——, C_L, C_N varying; – – –, C_L, C_N fixed, $C_L = 2{\cdot}255$, $C_N = 3{\cdot}317$, corresponding to $bk = n = 1$. The curve for $n = 3$ with C_L and C_N fixed is virtually identical with the curve for $n = 2$.

η itself being of little physical relevance. Indeed, a typical physically motivated definition of efficiency, say $C_L V^2 L/E$, would mask the variability of C_L and, therefore, not be as instructive for purposes of optimization. Equation (6.14) is plotted in figure 9, where we have again presented results for C_N and C_L variable and constant. The indication is that a single wavelength is preferable to two or more, except for small bk, where two wavelengths are better. For a given n there exists an optimum bk, which decreases as n increases. Of course the beat frequency kc and wave propagation speed vary in order for the swimming constraint to be satisfied. The composite optimum is $n = 1$ with $bk \doteqdot 1{\cdot}318$, corresponding to $\alpha \doteqdot 40°$, and at which $c/V = 8{\cdot}863$ and $\omega L/V = 72{\cdot}693$.

As a conclusion to this section, it is instructive to consider the extent to which the pitching of the flagellum, which is necessary to conserve angular momentum, affects the propulsive speed, rate of working and propulsive efficiency. Accordingly, we have in figure 10 compared these values with those for a flagellum artificially constrained to swim with a unidirectional velocity along the $-x$ axis. Figure 10 indicates that the assumption of unidirectional propulsion results in an overestimate of the swimming speed, a somewhat smaller underestimate of the rate of working and therefore an overestimate of the propulsive efficiency η. However, these discrepancies diminish rapidly with increasing n, and in fact, are not appreciable for $n \geqslant 2$. Moreover, the presence of a head, tending to damp the necessary pitching, will reduce them further. Consequently in the next section we shall consider the quantitative influence of the head, using the assumption of unidirectional swimming.

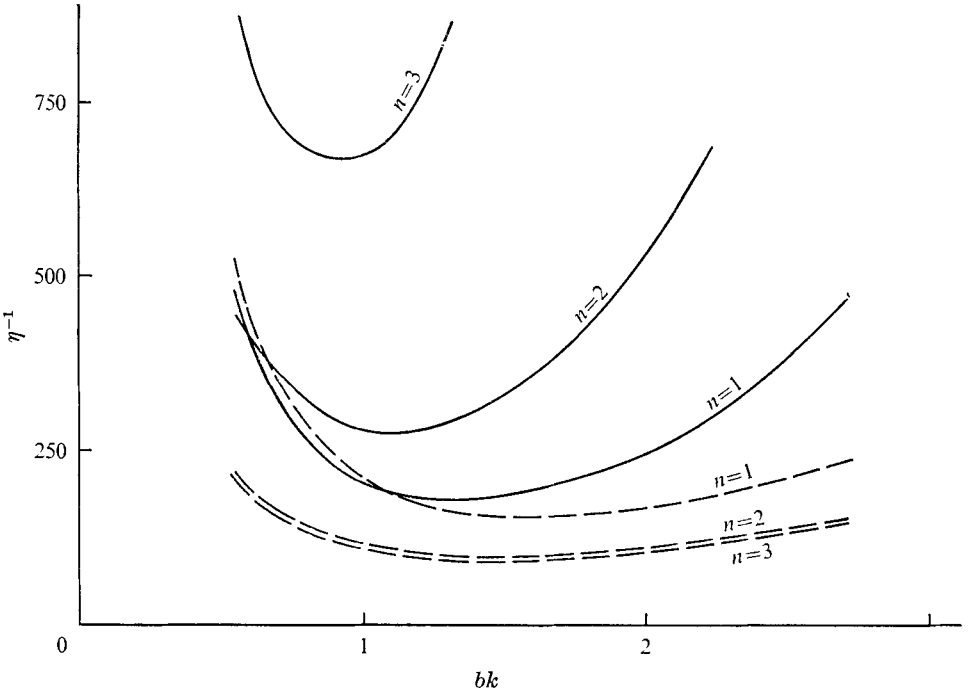

FIGURE 9. Reciprocal propulsive 'efficiency' for the sawtooth waves without a head. The scale of η^{-1} has no physical relevance. ——, C_L, C_N varying; – – –, C_L, C_N fixed.

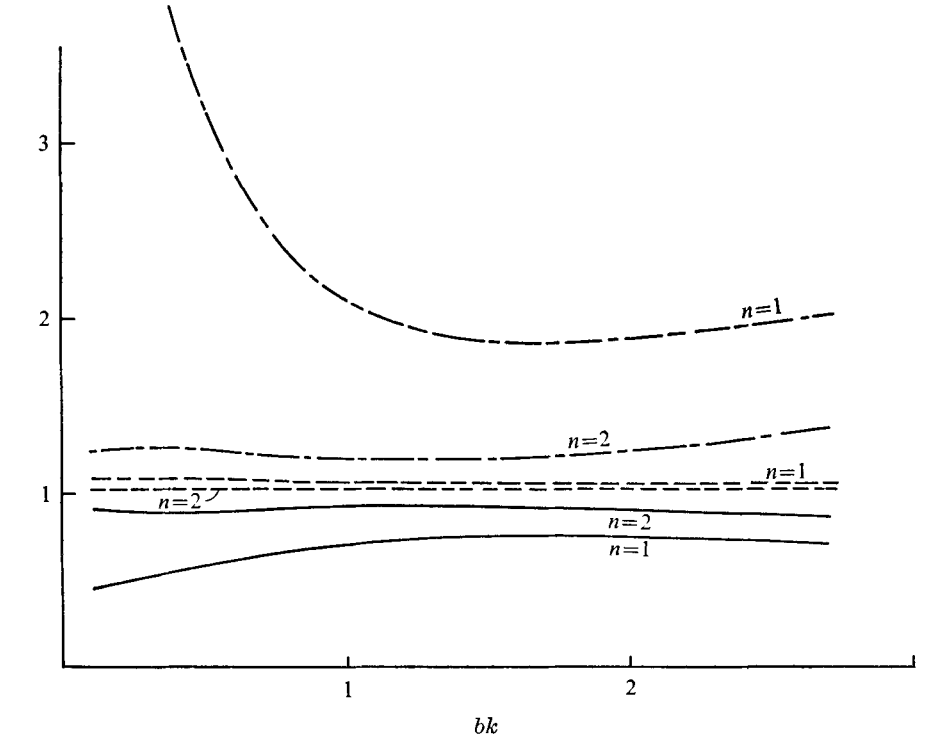

FIGURE 10. Comparison of results for headless sawtooth propulsion with and without conservation of angular momentum; the subscript u denotes unidirectional, meaning that angular momentum is not strictly conserved. ——, V/V_u; – – –, E/E_u; — · —, η^{-1}/η_u^{-1}.

7. Unidirectional propulsion with a head

In this section we consider a flagellum which has a head, rigidly attached to the forward end, and which propagates the two-dimensional periodic waves introduced previously. For the sake of convenience we consider a spherical head of radius a and we assume that a and n are sufficiently large that ω effectively vanishes. Thence $V_{pX} = V_{px}$, $V_{pY} = V_{py}$ and the solution of (5.6) and (5.7) becomes

$$\frac{V_{px}}{c} = \left[\frac{\gamma}{(\gamma-1)} - B + \frac{C_H^*}{(\gamma-1)L}\right]^{-1} \left\{1 - B + \frac{C_H^*}{(\gamma-1)L}[1 - A\cos\alpha(0,t)]\right\}, \quad (7.1)$$

$$\frac{V_{py}}{c} = -\left[\frac{1}{\gamma-1} + B + \frac{C_H^*}{(\gamma-1)L}\right]^{-1} \frac{C_H^*}{(\gamma-1)L}[A\sin\alpha(0,t)]. \quad (7.2)$$

Notably, if the time average of (7.1) and (7.2) is taken, the time-dependent terms vanish, and $\overline{V}_{px}$ reduces to the value considered by Lighthill (1974). Now the time-average rate of working by the organism can be written as

$$\frac{\overline{E}}{LC^2C_L} = [\gamma - B(\gamma-1)][(1-\overline{V}_{px})^2 + \overline{V_{px}^{*2}} - 2(1-\overline{V}_{px})] + \overline{V_{py}^2}[1 + B(\gamma-1)] + \overline{E}_H/Lc^2C_L, \quad (7.3)$$

where V_{px}^* is the time-dependent component of V_{px} and $\dot{E}_H = C_H\,\mathbf{v}(0,t).\mathbf{v}(0,t)$ is the rate of working associated with the movements of the head. The time average of $\dot{E}_H$ can be written as

$$\frac{\overline{E}_H}{Lc^2C_H} = \left(\frac{\overline{V}_{px}}{c}\right)^2 + \left[\frac{\gamma/(\gamma-1) - B}{\gamma/(\gamma-1) - B + C_H^*/(\gamma-1)L}\right]^2 \left[\frac{B}{A^2} - 1\right] + \left[\frac{(\gamma-1)^{-1} + B}{(\gamma-1)^{-1} + B + C_H^*/(\gamma-1)L}\right]^2 \left[\frac{1}{A^2}(1-B)\right]. \quad (7.4)$$

Of particular interest are the contributions of the unsteady components of the motion to $\overline{E}$, namely the terms in $\overline{V_{px}^{*2}}$ and $\overline{V_{py}^2}$ in (7.3), and the final two terms in (7.4). Sample computations based on the sawtooth beat of §6 indicate that throughout the range $0{\cdot}57 \leqslant bk \leqslant 2{\cdot}72$ (i.e. $20° \leqslant \alpha \leqslant 60°$) those unsteady motions increase $\overline{E}$ by 30–40 %.† This is not surprising if one notes that the surface area of the entire typical flagellum is $151\,\mu m^2$ while the area of the typical head is $113\,\mu m^2$. Therefore, it clearly behoves a micro-organism to limit as much as possible the twitching movements of its head. Indeed, this is precisely the indication of the general theory in §4, cf. (4.4) and (4.5). There the suggestion was that a wave envelope exponentially increasing away from the head is optimal. In the context of the purely periodic waves introduced here, the twitching of the head could be reduced by initiating the flagellar contractions at a point away from the junction between the head and the flagellum, and flexing the small intermediate segment of the flagellum between the two points

† Use of the optimally shaped sawtooth to quantify this unsteady effect provides, in fact, a conservative estimate since longitudinal movements relative to the axis, normally present in real flagella, vanish.

so as to keep the head still. Thence the periodic analysis would remain approximately valid. Moreover, a non-zero component of V_{py} would no longer be necessary to propel the flagellum periodically sideways, so as to balance the lateral forces acting on the head. Thus the traditional case of unidirectional propulsion would be approached, only with a slightly increased drag coefficient for the head.

It is not physiologically instructive to seek an optimization for the case of a fully twitching head. Lighthill (1974) has considered the limiting case in which $\mathbf{v}(0,t) = -V_p(t)$ and in which, consequently, the head has little effect on the rate of working. It is worth quoting his result that, if the variations in C_L and C_N with k are neglected, the optimum slope angle for the already optimally shaped sawtooth is $\alpha = 42°$, corresponding to $bk = 1{\cdot}467$, and with a variation of only a few per cent over a representative range of flagellar and head sizes. In so far as non-vanishing twitching movements of the head are concerned, it is unlikely that an optimum bk obtained for that case would differ significantly from the result here. Indeed, remembering the optimum $\alpha \doteqdot 40°$ obtained in § 6 for a headless pitching sawtooth with variable resistance coefficients, we may conclude that the neighbourhood of $\alpha = 42°$ is optimal for this form of propulsion.

8. Discussion

This paper has made an inquiry into the nature of flagellar undulations that are hydrodynamically optimal. The results of the qualitative study in §§ 2, 3 and 4 appear consistent with what is observed in nature. Uniflagellated micro-organisms span a considerable spectrum of development, from simple bacteria, to protozoa to spermatozoa, the mammalian spermatozoon being in fact one of the most sophisticated cells in nature. The suggestion in § 3 that under optimal conditions the entire flagellum assumes an active role in the propagation of wave-like undulations is not unreasonable biologically. For example, microscopic observation of fresh semen always reveals some organisms that do not actively use the entire flagellum. In some cases this aberrant behaviour is obviously pathological, while in other cases the implication is less clear. High speed cinemicrography suggests on a more precise level that the entire flagellum is not always active. Thus our result is a potentially useful criterion for visual assessment of organism motility.

The suggestion in § 4 of an exponentially growing wave envelope with reduced twitchings of the head is quite consistent with the motions of many higher spermatozoa. Indeed, the quantitative indication in § 7 that unrestrained head twitching can increase the energy expenditure by as much as 30–40 % does not appear to have been realized by previous investigators. Although these results are for two-dimensional undulations, the same conclusions very likely apply to three-dimensional flagellar waves.

Of course, many micro-organisms do propagate three-dimensional waves, to which (5.6)–(5.8) are not applicable in general. The preferability of this form of beat to the planar case appears to depend upon the size of the head, the wavelength and amplitude and the number of wavelengths. Chwang & Wu (1971) indicate that circular helical waves are preferable to sinusoidal waves of the same

wavelength and amplitude when $a/r_0 > 10$ (a being the radius of a spherical head and r_0 the radius of the flagellum); for $a/r_0 < 5$, the planar waves are better. Unfortunately a bull spermatozoon, for example, is characterized by $a/r_0 \doteqdot 7{\cdot}5$. Coakley & Holwill (1972) indicate that, for small wave amplitudes, helical waves (with elliptical cross-section of any eccentricity) are preferable to corresponding sinusoidal ones, the preference being reversed at large amplitudes. Their suggested transition region of $bk = 1$ again corresponds to what is often observed. Neither of these analyses, the latter of which does not conserve the rolling component of angular momentum, allows for variations in the resistance coefficients and conservation of transverse angular momentum. Moreover, in both cases the twitching motions of the head are omitted. It is possible that these latter two considerations would affect a comparison of two- and three-dimensional wave forms.

It should be noted that there is no inconsistency in our result for small amplitude waves that for the sinusoidal shape one wavelength is preferable, whereas for the sawtooth two wavelengths are better. For equivalent bk and c, the sinusoid pitches less than the sawtooth, and consequently does not require a second wavelength to reduce such motions and maximize efficiency. This is not unreasonable if one considers the increased pitching moments likely to be generated near the sharp bends of the sawtooth and remembers that for small amplitudes the wave fronts of the sinusoid are themselves quite flat. In fact the sinusoid swims faster than the sawtooth, for any n, but with a sufficiently higher rate of working that the trade-off with propulsive velocity is not hydrodynamically optimal. Indeed, for fixed bk and given propulsive velocity, the sinusoid must beat faster than the sawtooth. These relative tendencies deserve study for waves of finite amplitude and the authors are at present engaged in a numerical investigation of them, as well as of other questions raised throughout this discussion.

The results in §6 for finite amplitude sawtooth waves do, in fact, indicate that one wavelength is preferable to two or more; and the presence of a head would reinforce this tendency. Of course, we have for mathematical convenience restricted our study to integral numbers of wavelengths. It is possible that an imbalance created by a non-integral number of wavelengths could help to reduce the energy expenditure due to the head. Among higher spermatozoa, the effective number of wavelengths tends to be between one and two, a rough average being perhaps 1·4.

We have in §6 cautioned that the accuracy of the expressions for C_N and C_L probably diminishes with increasing wave amplitude. Thus our curves for $\overline{V}_{pX}$, $\overline{E}$ and η^{-1}, cf. figures 7–9, which we have purposely extended to unreliably high values of bk, should in fact tend to flatten out at such high values. The preferability of one wavelength over two begins to manifest itself for the sawtooth around $bk = 0{\cdot}5$, and therefore is as accurate as are our expressions for C_N and C_L from that value upwards. Proper treatment of this difficulty requires more fundamental application of the methods of slender-body theory.

Notably, direct numerical investigation of the basic optimization problem in §3 should account for this variability of C_N and C_L. However, even for fixed C_N and C_L that problem is inherently unstable, as can be inferred from our ana-

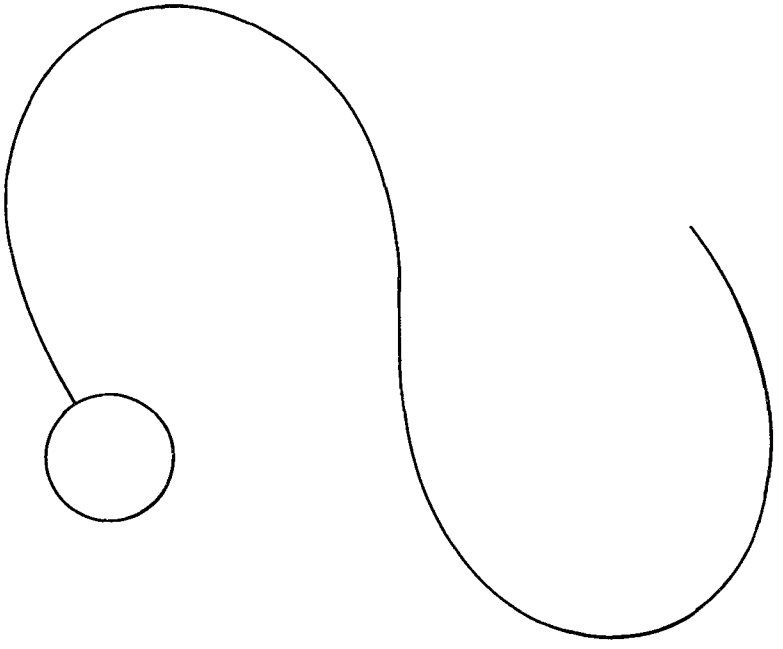

FIGURE 11. A flagellar wave form shaped like a 'meander', after Silvester & Holwill (1972).

lytical study. The integration of (2.14) and (2.15) with respect to time, say by a high-order Runge–Kutta scheme, is extremely sensitive to errors in the numerical specification of ξ_0. More important, the extension $\tilde{\xi}_0$ determined by the computer is generally the analytical extension. If after any time step this extension should fail to satisfy the compatibility criteria discussed in §3, propulsion would be impossible at that instant and the problem would break down.

Finally, it is worth commenting briefly on the relationship of our hydrodynamical study to the internal dynamics of flagella. Silvester & Holwill (1972) have noted that the elastic potential energy of a slender rod is proportional to

$$\int_0^L \frac{ds}{R^2}$$

and that the shape which minimizes this energy, which they term a 'meander', closely resembles the wave forms of some flagella; see figure 11. Thus the tendency towards flat wave fronts, e.g. on the sawtooth, may be structurally beneficial. A hydroelastic optimization problem can be posed. However, we should stress that recent developments in the study of the contraction mechanism emphasize the importance of the active internal processes involved. We might add though that, as such studies achieve increased levels of sophistication, allowance for the variability of the resistance coefficients should be considered.

The authors are grateful for general comments from Professor Sir James Lighthill, and for suggestions on the ill-fated numerical aspects of the optimal

control problem from Dr P. Kemp. D. F. K. acknowledges a Population Council Postdoctoral Fellowship.

Appendix

The coefficients in (6.5)–(6.11) for propulsion by sawtooth waves may be expressed as follows:

$$F_1 = \left(\frac{\gamma}{\gamma-1} - B\right)\left[\frac{\gamma}{\gamma-1} + 2B + \left(\frac{\pi n}{bk}\right)^2\left(\frac{8\gamma-7}{\gamma-1} - 7B\right)\right],$$

$$G_1 = 3B\,[B - (2\gamma-1)/(\gamma-1)],$$

$$F_2 = \left(\frac{1-B}{\gamma/(\gamma-1)-B}\right)F_1,$$

$$G_2 = \left[\frac{[B(\gamma-1)]^{-1}+2B}{(2\gamma-1)/(\gamma-1)-B}\right]G_1, \quad G_5 = \left[\frac{\gamma/(\gamma+1)^2+1-B^2}{B[(2\gamma-1)/(\gamma-1)-B]}\right]G_1,$$

$$G_3 = -(\pi nA/bk)\,G_5, \quad G_4 = -(2\pi n/bk)\,G_5,$$

where $B = A^2 = (2\pi n/kL)^2$ and $\gamma = C_N/C_L$.

REFERENCES

Brokaw, C. J. 1972 Computer simulation of flagellar movement. *Biophys. J.* **12**, 564.

Coakley, C. J. & Holwill, M. E. J. 1972 Propulsion of microorganisms by three dimensional flagellar waves. *J. Theor. Biol.* **35**, 525.

Chwang, A. T. & Wu, T. Y. 1971 A note on the helical movement of microorganisms. *Proc. Roy. Soc.* B **178**, 327.

Cox, R. G. 1970 The motion of long slender bodies in a viscous fluid. Part 1. General theory. *J. Fluid Mech.* **44**, 791.

Gray, J. & Hancock, G. J. 1955 The propulsion of sea urchin spermatozoa. *J. Exp. Biol.* **44**, 578.

Hancock, G. J. 1953 The self-propulsion of microscopic organisms through fluids. *Proc. Roy. Soc.* A **217**, 96.

Lighthill, M. J. 1974 *Mathematical Biofluiddynamics.* S.I.A.M.

Lions, J. L. 1968 *Optimal Control of Systems Governed by Partial Differential Equations.* Springer.

Machin, K. E. 1958 Wave propagation along flagella. *J. Exp. Biol.* **35**, 796.

Machin, K. E. 1963 The control and synchronization of flagellar movement. *Proc. Roy. Soc.* B **158**, 88.

Pontryagin, Boltyanskii, Gamkzelidze & Mishchenko 1962 *The Mathematical Theory of Optical Processes.* Interscience.

Shack, W. J., Fray, C. S. & Lardner, T. J. 1971 Observations on the hydrodynamics and swimming motions of mammalian spermatozoa. *Preprint Dept. Mech. Engng, M.I.T.*

Silvester, N. R. & Holwill, M. E. J. 1972 An analysis of hypothetical flagellar waveforms. *J. Theor. Biol.* **35**, 505.

Taylor, G. I. 1951 Analysis of swimming of microorganisms. *Proc. Roy. Soc.* A **209**, 477.

Taylor, G. I. 1952 The action of waving cylindrical tails in propelling microscopic organisms. *Proc. Roy. Soc.* A **211**, 225.